

**Supporting Information
for**

**Towards atomic resolution in sodium titanate nanotubes
using near-edge X-ray-absorption fine-structure
spectromicroscopy combined with multichannel multiple-
scattering calculations**

**Carla Bittencourt^{*1}, Peter Krüger², Maureen J. Lagos³, Xiaoxing Ke³, Gustaaf Van
Tendeloo³, Chris Ewels⁴, Polona Umek^{5,6} and Peter Guttmann⁷**

Address: ¹ChIPS, University of Mons, B-7000, Mons, Belgium, ² ICB, UMR 6303 CNRS-Université de Bourgogne, F-21078 Dijon, France, ³EMAT, University of Antwerp, B-2020, Antwerp, Belgium, ⁴ Institut des Matériaux de Nantes (IMN), Université de Nantes, CNRS, Nantes, France, ⁵Jožef Stefan Institute, Jamova cesta 39, 1000 Ljubljana, Slovenia, ⁶Center of Excellence NAMASTE, Jamova cesta 39, 10000 Ljubljana, Slovenia and ⁷Helmholtz-Zentrum Berlin für Materialien und Energie GmbH, Institute for Soft Matter and Functional Materials, Albert-Einstein-Str. 15, 12489 Berlin, Germany

Email: Carla Bettencourt* - carla.bittencourt@umons.ac.be

*Corresponding author

Broadening of the O K-edge spectra, comparison of the XPS Ti spectra recorded on the anatase and on the (Na,H)TiNTs, and experimental details.

Broadening of the O K-edge spectra

Following the prescription used in the MXAN code [1] the O-K edge spectra were broadened with a Lorentzian function of energy-dependent width $\Gamma(E)=\Gamma_c+A_s(0.5 + \arctan((E-E_s)/b)/\pi)$. Here Γ_c is the natural width of the O 1s hole (0.156 eV) and E_s is the step position, which was taken as the plasmon peak of anatase (12.7 eV) [2]. The parameters $A_s = 1$ eV (step height) and $b = 2$ eV have been adjusted to the experiment. The same parameter values were used for anatase and the (Na,H)TiNTs.

XPS study of the sample

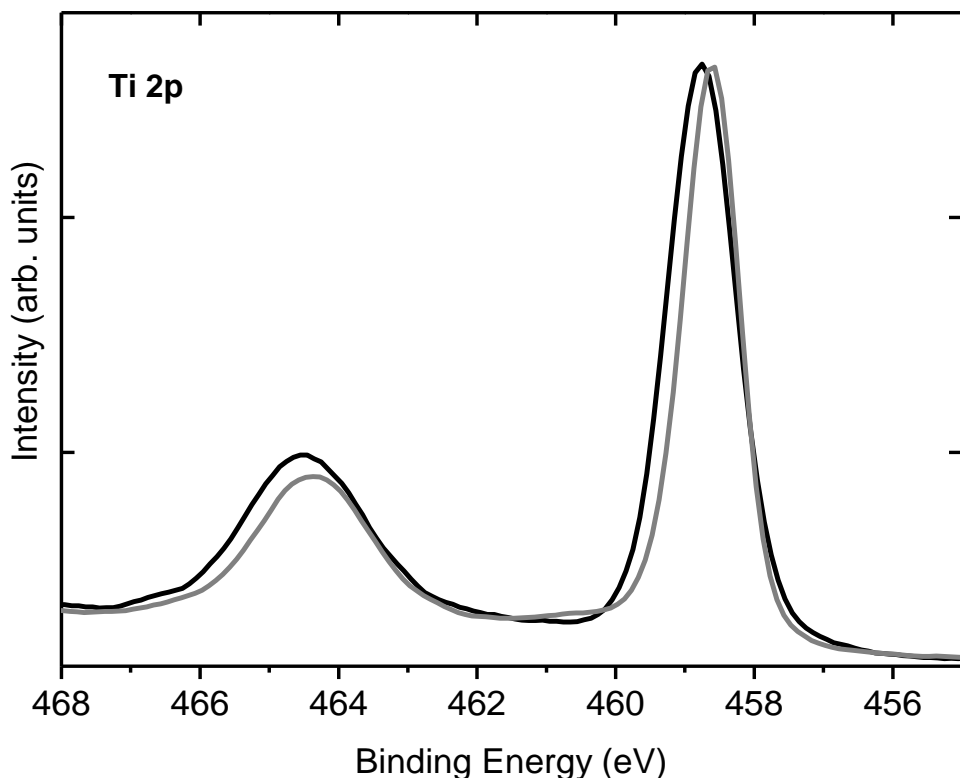


Figure S1: Comparison of the Ti 2p XPS core-level spectra recorded on (Na,H)TiNTs (grey line) and on anatase (black line) reference powder used as starting material.

Experimental

Materials Sodium titanate nanotubes ((Na,H)TiNTs) were synthesized from TiO₂ microparticles and NaOH(aq) under hydrothermal conditions at 135 °C. Detailed experimental procedure is described in [3]. Elemental composition (excluding hydrogen) determined with electron dispersive spectrometry (EDS) in combination with scanning electron microscopy (SEM) shows sodium content of 11.2 wt %, titanium 45.3 wt % and oxygen 43.5 wt %, respectively. Our XPS measurements show the samples to be about 10 wt % intercalated Na, in agreement with the EDS values.

Characterization The morphology of the synthesized material was investigated with a TEM (Jeol 2100 and a Tecnai G2 at 200 kV). For TEM and NEXAFS–TXM analysis the nanotubes were sonically dispersed in ethanol and a drop of the solution was deposited onto a lacey carbon film supported by a copper grid. Note that due to electron-beam damage effects on the (Na,H)TiNTs, different grids were used for the electron microscopy and for the NEXAFS–TXM analysis.

The Ti 2p L-edge spectra were recorded with the TXM installed at the undulator beamline U41-XM at BESSY II, Berlin [4-6]. The setup of the instrument is analogous to a bright-field light microscope. A focusing spherical grating monochromator (FSGM) at the undulator beamline U41-XM at the electron storage ring BESSY II of the HZB delivers X-rays with photon energy E and the required high spectral resolution of $E/\Delta E \geq 4500$. A single reflection ellipsoidal shaped mirror condenser [7,4] is used to illuminate an object field of 15–20 μm .

In the best case the HZB TXM provides a high spatial resolution close to 10 nm (half-pitch) [8] and a spectral resolution up to $E/\Delta E \approx 10^4$. It allows measurements to be taken at room or liquid nitrogen temperature in a vacuum of 10^{-7} TORR. The spectra were recorded at room temperature in transmission mode by taking a sequence of images over a range of photon energies covering the investigated absorption edges with $E/\Delta E \geq 4500$. Note that the exit slit of the monochromator was set to 5 μm , which corresponds to a calculated spectral resolution of $E/\Delta E = 2 \times 10^4$. For the present study a zone plate objective with an outermost zone width of 40 nm was used to image the sample onto a cooled back-illuminated soft X-ray CCD camera (Roper Scientific, PI SX1300).

The NEXAFS spectra were normalized since the photon flux varies as a function of photon energy ($h\nu$) and time in the object field (x, y). The normalization was performed by dividing the function $I(x, y, h\nu)$ recorded on the sample by the photon flux curve $I_o(x + \Delta x, y + \Delta y, h\nu)$

recorded in its sample free proximity at position $(x + \Delta x, y + \Delta y)$. Both $I(x, y, h\nu)$ and $I_o(x, y, h\nu)$ were recorded in the same image stack since near each studied nanostructure bare regions permit the measurement of I_o .

The elemental compositions of the sample was investigated with a FE-SEM (Carl Zeiss, Supra 35 LV) equipped with an EDS (energy-dispersive X-ray spectrometer) element analysis system. XPS (X-ray photoelectron spectroscopy) measurements were also performed to determine chemical composition, in a VERSAPROBE PHI 5000 from Physical Electronics, equipped with a monochromatic Al K α X-ray source with a highly focused beam size that can be set from 10 to 300 μm . The energy resolution was 0.6 eV. For the compensation of the built up charge on the sample surface during the measurements, a dual-beam charge neutralization composed of an electron gun (~ 1 eV) and argon ion gun (≤ 10 eV) was used. The relative amount of sodium was evaluated to be 12% in accordance with EDS (11%).

References

1. Benfatto, M.; Della Longa, S.; D'Angelo, P. *Phys. Scr.* **2005**, *T115*, 28–30. doi:10.1238/Physica.Topical.115a00028
2. Mo, S.-D.; Ching, W. Y. *Phys. Rev. B* **1995**, *51*, 13023–13032. doi:10.1103/PhysRevB.51.13023
3. Umek, P.; Cevc, P.; Jesih, A.; Gloter, A.; Ewels, C. P.; Arcon, D. *Chem. Mater.* **2005**, *17*, 5945–5950. doi:10.1021/cm050928w
4. Guttmann, P.; Zeng, X.; Feser, M.; Heim, S.; Yun, W.; Schneider, G. *J. Phys.: Conf. Ser.* **2009**, 012064–012066.
5. Schneider, G.; Guttmann, P.; Heim, S.; Rehbein, S.; Mueller, F.; Nagashima, K.; Heymann, J. B.; Muller, W. G.; McNally, J. G. *Nat. Methods* **2010**, *7*, 985–987. doi:10.1038/nmeth.1533
6. Guttmann, P.; Bittencourt, C.; Rehbein, S.; Umek, P.; Ke, X.; Van Tendeloo, G.; Ewels, C. P.; Schneider, G. *Nat Photon* **2012**, *6*, 25–29.
7. Zeng, X.; Duewer, F.; Feser, M.; Huang, C.; Lyon, A.; Tkachuk, A.; Yun, W. *Appl. Opt.* **2008**, *47*, 2376–2381. doi:10.1364/AO.47.002376
8. Rehbein, S.; Guttmann, P.; Werner, S.; Schneider, G. *Opt. Express* **2012**, *20*, 5830–5839. doi:10.1364/OE.20.005830